23rd International Symposium on Mathematical Theory of Networks and Systems
Hong Kong University of Science and Technology, Hong Kong, July 16-20, 2018

Structured Discretization of the Heat Equation: Numerical Properties and Preservation of Flatness

Paul Kotyczka[1]

***Abstract*— We show the application of a recently presented structure-preserving semi-discretization method to the heat equation on an arbitrary dimensional spatial domain. It retains the separation of the geometric (Stokes-)Dirac structure with its global balance equation, from the dynamics and constitutive equations. On the 1D example, we exploit the banded structure of the resulting state space matrices in order to analyze the approximation quality of the eigenvalues for two representative parametrizations. We show that the spatial discretization scheme preserves also a given flat output as a basis for feedforward motion planning.**

I. INTRODUCTION

The *port-Hamiltonian* (PH) framework offers a structured and unifying approach, among others for the modeling of conservation laws, including heat transfer and thermodynamic systems [1]. Focusing the attention to conservation laws, a salient feature of the PH approach is that very different physical systems share a common geometric structure [2]. This *so-called Stokes-Dirac* structure involves a *canonical* differential operator (up to possibly different signs which distinguish the *hyperbolic* from the *parabolic* case). It is directly related with a *balance equation* that holds independently of the actual dynamics and constitutive equations. Substituting the latter gives e. g. the global balance of flows of energy or entropy. The heat equation, which is considered in this paper, can be represented in terms of two first order differential equations in space for a) the conservation of internal energy and b) the thermodynamic driving force. Fourier's law and a calorimetric relation close the system representation.

A first approach to a *structure-preserving* spatial discretization that separates the linear (Stokes-)Dirac structure from the constitutive and dynamics equations was presented in [3] and applied, among others, successfully to diffusive processes [4]. A main feature of this *mixed finite element* like approach is that the differential relations between the *dual* system variables (so-called *flows* and *efforts*) are *exactly* satisfied in the approximation bases. In the same spirit, a *geometric* pseudo-spectral method was presented in [5]. The mixed discretization of the structure equations in both approaches leads to a *degenerate* duality product between the discrete flow and effort degrees of freedom. The degeneracy is resolved by defining *reduced effort vectors* such that the overall discrete balance equation can be expressed via non-degenerate pairings of flows and reduced efforts. Drawbacks of the approach in [3] are that the extension to higher spatial dimensions is not obvious and that the representation of the system equations in strong form restricts the degrees of freedom in the *power-preserving* effort maps.

In [6], we presented a new approach for the spatial discretization of PH systems of conservation laws, which is based on the *weak form* of the Stokes-Dirac structure. By *parametrized* linear maps of the *flow* degrees of freedom (in contrast to the efforts as described above), the method is applicable to arbitrary spatial dimension. While preserving the geometric structure (a finite-dimensional *Dirac structure* approximates the infinite-dimensional Stokes-Dirac structure), different parametrizations of the resulting numerical models are possible, adapted to the nature of the considered problem: A parameter choice in the sense of *upwinding* is favorable for hyperbolic systems [6], while parabolic systems like the heat equation in the present paper are better approximated using a parametrization which corresponds to a *centered* approximation of the constitutive equations.

In this paper, we summarize the application of this method to the nD heat equation. We present the resulting matrices for the 1D case and an approximation based on Whitney forms [7]. The tridiagonal structure of the discretized system matrices for two parametrizations allows for an explicit computation of the discretized eigenvalues. The "centered" approximation with $\alpha = \frac{1}{2}$ turns out to be second order accurate, while the "one-sided" approximation with $\alpha = 0$ is only first order accurate[1]. In both cases, the structure of the discretized models allows for a *flat parametrization* of the control input in terms of a given desired output and its time derivatives. This is a property, which is preserved from the infinite-dimensional model, see [9] for the flatness-based motion planning of the 1D heat equation.

The remainder of the paper is structured as follows. In Section II, we introduce the representation of the heat equation in terms of a Stokes-Dirac structure, constitutive and dynamics equations. In Section III, we show step by step the application of the structure-preserving discretization according to [6] to the nD heat equation. Section IV is devoted to the concrete representation of the resulting system matrices in the 1D case. In Section V, the two considered parametrizations are analyzed in terms of their eigenvalue approximation and the preservation of the given flat output. Simulation results illustrate the theoretical findings. Section

*The work is supported by Agence Nationale de la Recherche-Deutsche Forschungsgemeinschaft (ANR-DFG), project INFIDHEM, ID ANR-16-CE92-0028 and Deutsche Forschungsgemeinschaft, project KO 4750/1-1.

[1]Paul Kotyczka is with the Department of Mechanical Engineering, Chair of Automatic Control, Technical University of Munich, Boltzmannstr. 15, 85748 Garching, Germany kotyczka@tum.de

[1]For this case, the model and the calculations coincide with the ones in [8] for the corresponding parameter choice in the approach [3].

VI concludes the paper with a summary and comments on ongoing work.

II. STRUCTURED REPRESENTATION OF THE HEAT EQUATION

A. Heat equation in arbitrary dimension

We consider the following structured model of the heat equation on an n-dimensional open domain Ω, $n \in \{1,2,3\}$. All quantities are *differential* forms of corresponding degree, see [10] for an introduction. $\Lambda^k(\Omega)$ denotes the space of smooth differential k-forms on Ω. The symbol d represents the *exterior derivative*, which maps a k-form to a $(k+1)$-form and allows for a generalized treatment of the different differential operators from vector calculus. The Hodge star $*$ maps k-forms to $(n-k)$-forms, which are associated to dual geometric objects[2]. Heat conduction, see [1], Sections 4.1.1 and 4.2.2, can be described by the *conservation law*

$$\frac{\partial u}{\partial t} = -\mathrm{d}J_Q \tag{1}$$

for the internal energy density $u \in \Lambda^n(\Omega)$ with the heat flux $J_Q \in \Lambda^{n-1}(\Omega)$. The latter can be described phenomenologically by Fourier's law

$$J_Q = - * (\lambda(T)F) \tag{2}$$

with $\lambda(T) \in \Lambda^0$ the heat conductivity and $F \in \Lambda^1(\Omega)$ the thermodynamic driving force

$$F = dT, \tag{3}$$

which corresponds to the temperature gradient. The differential relation between internal energy density and temperature shall be expressed by

$$\delta u = *c_v(T)\delta T \tag{4}$$

with $c_v(T) \in \Lambda^0(\Omega)$ the isochoric heat capacity.

B. Structure equations, Stokes-Dirac structure

Defining the *flow* and *effort* variables

$$f^p = -\frac{\partial u}{\partial t}, \quad f^q = F, \quad e^p = T, \quad e^q = (-1)^{n-1}J_Q, \tag{5}$$

we observe the purely linear relation

$$\begin{bmatrix} f^p \\ f^q \end{bmatrix} = \begin{bmatrix} 0 & (-1)^{n-1}\mathrm{d} \\ \mathrm{d} & 0 \end{bmatrix} \begin{bmatrix} e^p \\ e^q \end{bmatrix} \tag{6}$$

between them, independent of any (material) parameter. The factor $(-1)^{n-1}$ is in analogy to the hyperbolic case and guarantees the formal skew symmetry of the differential operator for arbitrary n [2]. Flow and effort variables can be paired via a *duality product* between differential forms of appropriate degree on Ω

$$\langle \alpha | \beta \rangle_\Omega := \int_\Omega \alpha \wedge \beta, \qquad \alpha \in \Lambda^k(\Omega), \beta \in \Lambda^{n-k}(\Omega), \tag{7}$$

[2]The Hodge star induces an inner product on the space of differential forms on a manifold Ω. Or *vice versa*, a given inner product space induces the corresponding Hodge star, which is clearly a *metric-dependent* operation.

with $\wedge : \Lambda^k(\Omega) \wedge \Lambda^l(\Omega) \rightarrow \Lambda^{k+l}(\Omega)$ the antisymmetric wedge product. By the identities $\lambda \wedge \mu = (-1)^{kl}\mu \wedge \lambda$ and $\mathrm{d}(\lambda \wedge \mu) = \mathrm{d}\lambda \wedge \mu + (-1)^k \lambda \wedge \mathrm{d}\mu$ for any $\lambda \in \Lambda^k(\Omega)$, $\mu \in \Lambda^l(\Omega)$ and Stokes' theorem for differential forms $\int_\Omega \mathrm{d}\omega = \int_{\partial\Omega} \mathrm{tr}\,\omega$ for any $\omega \in \Lambda^{n-1}(\Omega)$, the following identity can be verified:

$$\langle e^p | f^p \rangle_\Omega + \langle e^q | f^q \rangle_\Omega + (-1)^n \langle \mathrm{tr}\, e^q | \mathrm{tr}\, e^p \rangle_{\partial\Omega} = 0. \tag{8}$$

The trace operator tr defines the restriction of functions defined on an *open* set Ω to its boundary $\partial\Omega$. The trace theorems, see e. g. [11], Section 9.8, and for differential forms [12], Section 4, clarify the functional spaces of these restrictions to the boundary. In the following, we consider $f^p \in L^2\Lambda^n(\Omega)$, $f^q \in L^2\Lambda^1(\Omega)$ and $e^p \in H^1\Lambda^0(\Omega)$, $e^q \in H^1\Lambda^{n-1}(\Omega)$, i. e. the flow differential forms with coefficient functions from the Lebesgue space L^2 and the effort differential forms from the Sobolev space H^1. For compactness of notation, we will omit the trace symbol in the sequel, i. e. $\langle e^q | e^p \rangle_{\partial\Omega} := \langle \mathrm{tr}\, e^q | \mathrm{tr}\, e^p \rangle_{\partial\Omega}$.

Defining as *boundary effort and flow*

$$e^\partial = (-1)^n \mathrm{tr}\, e^q \in L^2\Lambda^{n-1}(\partial\Omega), \quad f^\partial = \mathrm{tr}\, e^p \in L^2\Lambda^0(\partial\Omega), \tag{9}$$

the balance equation (8) reads

$$\langle f^p | e^p \rangle_\Omega + \langle f^q | e^q \rangle_\Omega + \langle f^\partial | e^\partial \rangle_{\partial\Omega} = 0. \tag{10}$$

The subspace of $\mathcal{F} \times \mathcal{E}$ with $\mathcal{F} = L^2\Lambda^n(\Omega) \times L^2\Lambda^1(\Omega) \times L^2\Lambda^0(\partial\Omega)$ and $\mathcal{E} = H^1\Lambda^0(\Omega) \times H^1\Lambda^{n-1}(\Omega) \times L^2\Lambda^{n-1}(\partial\Omega)$ of flows and efforts that satisfy (6) and (9) contains *exactly* those flows and efforts which satisfy balance equation (10). This subspace is called a *Stokes-Dirac structure*, see [2].

Remark 1: The Stokes-Dirac structure is the underlying geometric structure for the port-Hamiltonian formulation of *hyperbolic* systems of two conservation laws [2]. For those systems, (10) is a power balance, which represents energy conservation. For the heat equation as an example for a *parabolic* system, this interpretation does not hold. However, by the slightly different choice of variables $e^p = \frac{\delta S}{\delta u} = \frac{1}{T}$ and $f^q = -F'$ with F' the driving force in terms of $\frac{1}{T}$, (10) becomes a balance equation for the entropy $S = \int_\Omega s$ with a non-negative entropy generation term, see [1], Section 4.2.2.

Remark 2: The boundary term in (10) can be split in two, if $\partial\Omega$ is decomposed into regions Γ, where $e^\partial = (-1)^n \mathrm{tr}\, e^q$ is imposed as a boundary input and $\hat{\Gamma}$, where $\hat{e}^\partial = \mathrm{tr}\, e^p$ plays this role (the boundary variables have different *causality*):

$$(-1)^n \langle \mathrm{tr}\, e^q | \mathrm{tr}\, e^p \rangle_{\partial\Omega} = \langle f^\partial | e^\partial \rangle_\Gamma + \langle \hat{f}^\partial | \hat{e}^\partial \rangle_{\hat{\Gamma}}. \tag{11}$$

C. Constitutive equations and dynamics

With $p = u$ as conserved quantity and

$$e^q = (-1)^n \lambda(e^p) * f^q, \quad \mathrm{d}e^p = \frac{1}{c_v(e^p)} \mathrm{d}(*p), \tag{12}$$

the constitutive equations (2) and (4) in terms of the variables in (5), we obtain the differential equation

$$\frac{\partial e^p}{\partial t} = \frac{\lambda(e^p)}{c_v(e^p)} * \mathrm{d} * \mathrm{d}\, e^p, \tag{13}$$

which is the familiar representation of the heat equation in terms of the temperature $e^p = T$ with $*\mathrm{d} * \mathrm{d} = \mathrm{div}\,\mathrm{grad}$ the *Laplace-Beltrami* operator, see [13], Section 3.7.

III. MIXED GALERKIN STRUCTURE-PRESERVING APPROXIMATION

A. Discretization of the structure

We summarize the approach presented in [6] to discretize the structure equations (6), (9) such that the finite-dimensional subspace of *discrete flows and efforts* represents a *Dirac structure*. The elements of the Dirac structure are *exactly* the flow and effort vectors that satisfy the finite-dimensional counterpart of the balance equation (10).

1. The structure equations (6) in *weak form* are

$$\begin{aligned} \langle v^p | f^p \rangle_\Omega &= (-1)^{n-1} \langle v^p | \mathrm{d} e^q \rangle_\Omega \\ \langle v^q | f^q \rangle_\Omega &= \langle v^q | \mathrm{d} e^p \rangle_\Omega \end{aligned} \tag{14}$$

with $v^p \in H^1\Lambda^0(\Omega)$ and $v^q \in H^1\Lambda^{n-1}(\Omega)$ arbitrary weakly differentiable test forms. Integration by parts yields

$$\begin{aligned} \langle v^p | f^p \rangle_\Omega &= (-1)^n \langle \mathrm{d} v^p | e^q \rangle_\Omega - (-1)^n \langle\, v^p |\, e^q \rangle_{\partial\Omega} \\ \langle v^q | f^q \rangle_\Omega &= (-1)^n \langle \mathrm{d} v^q | e^p \rangle_\Omega - (-1)^n \langle\, v^q |\, e^p \rangle_{\partial\Omega}. \end{aligned} \tag{15}$$

2. For the *mixed Galerkin* approximation of the structure equations (15), we choose flow, effort and test differential forms from the finite-dimensional subspaces

$$\begin{aligned} f_h^p &\in \mathrm{span}\{\psi_1^p, \dots, \psi_{N_p}^p\} \subset L^2\Lambda^n(\Omega), \\ f_h^q &\in \mathrm{span}\{\psi_1^q, \dots, \psi_{N_q}^q\} \subset L^2\Lambda^1(\Omega) \end{aligned} \tag{16}$$

and

$$\begin{aligned} e_h^p, v_h^p &\in \mathrm{span}\{\varphi_1^p, \dots, \varphi_{M_p}^p\} \subset H^1\Lambda^0(\Omega), \\ e_h^q, v_h^q &\in \mathrm{span}\{\varphi_1^q, \dots, \varphi_{M_q}^q\} \subset H^1\Lambda^{n-1}(\Omega). \end{aligned} \tag{17}$$

We summarize the basis forms in the vectors $\boldsymbol{\psi}^p \in L^2\Lambda^n(\Omega; \mathbb{R}^{N_p})$, $\boldsymbol{\psi}^q \in L^2\Lambda^1(\Omega; \mathbb{R}^{N_q})$, $\boldsymbol{\varphi}^p \in H^1\Lambda^0(\Omega; \mathbb{R}^{M_p})$ and $\boldsymbol{\varphi}^q \in H^1\Lambda^{n-1}(\Omega; \mathbb{R}^{M_q})$. In order to have the structure equations (6) *exactly* satisfied in the approximation spaces, we require the *compatibility conditions* (in the weak sense)

$$\begin{aligned} \mathrm{span}\{\psi_1^p, \dots, \psi_{N_p}^p\} &= \mathrm{span}\{\mathrm{d}\varphi_1^q, \dots, \mathrm{d}\varphi_{M_q}^q\}, \\ \mathrm{span}\{\psi_1^q, \dots, \psi_{N_q}^q\} &= \mathrm{span}\{\mathrm{d}\varphi_1^p, \dots, \mathrm{d}\varphi_{M_p}^p\}. \end{aligned} \tag{18}$$

Such approximation spaces, whose sequences form subcomplexes of the de Rham complex, can be constructed in a variety of ways, see for finite elements [14]. The simplest case, which we shall consider in this paper, is the complex of the famous *Whitney forms* [7].

Substitute $f_h^p = \langle \mathbf{f}^p | \boldsymbol{\psi}^p \rangle$, $f_h^q = \langle \mathbf{f}^q | \boldsymbol{\psi}^q \rangle$, $e_h^p = \langle \mathbf{e}^p | \boldsymbol{\varphi}^p \rangle$, $e_h^q = \langle \mathbf{e}^q | \boldsymbol{\varphi}^q \rangle$, $v_h^p = \langle \mathbf{v}^p | \boldsymbol{\varphi}^p \rangle$ and $v_h^q = \langle \mathbf{v}^q | \boldsymbol{\varphi}^q \rangle$ in (15) with $\mathbf{f}^p \in \mathbb{R}^{N_p}$, $\mathbf{f}^q \in \mathbb{R}^{N_q}$, $\mathbf{e}^p, \mathbf{v}^p \in \mathbb{R}^{M_p}$ and $\mathbf{e}^q, \mathbf{v}^q \in \mathbb{R}^{M_q}$ the vectors of degrees of freedom and $\langle \cdot | \cdot \rangle$ the standard scalar product. The equations must hold for all $\mathbf{v}^p \in \mathbb{R}^{M_p}$ and $\mathbf{v}^q \in \mathbb{R}^{M_q}$, which yields two matrix equations of the form

$$\begin{aligned} \mathbf{M}_p \mathbf{f}^p + (\mathbf{K}_p + \mathbf{L}_p)\mathbf{e}^q &= \mathbf{0}, \\ \mathbf{M}_q \mathbf{f}^q + (\mathbf{K}_q + \mathbf{L}_q)\mathbf{e}^p &= \mathbf{0}. \end{aligned} \tag{19}$$

Assuming factorizations of the matrices $\mathbf{K}_p + \mathbf{L}_p = -(-1)^{n-1}\mathbf{M}_p\mathbf{d}_p$ and $\mathbf{K}_q + \mathbf{L}_q = -\mathbf{M}_q\mathbf{d}_q$, the discrete counterpart of the structure equation (6) becomes

$$\begin{bmatrix} \mathbf{f}^p \\ \mathbf{f}^q \end{bmatrix} = \begin{bmatrix} \mathbf{0} & (-1)^{n-1}\mathbf{d}_p \\ \mathbf{d}_q & \mathbf{0} \end{bmatrix} \begin{bmatrix} \mathbf{e}^p \\ \mathbf{e}^q \end{bmatrix}. \tag{20}$$

In the considered case of Whitney forms, $\mathbf{d}_p \in \mathbb{R}^{N_p \times M_q}$ and $\mathbf{d}_q \in \mathbb{R}^{N_q \times M_p}$ are the *co-incidence matrices* that relate the oriented n-simplices of the triangular discretization mesh with the n–1-simplices and the directed edges with the nodes.

3. The effort degrees of freedom that correspond to *imposed boundary conditions*, i. e. system *inputs*, are isolated from the vectors $\mathbf{e}^p$ and $\mathbf{e}^q$ by

$$\mathbf{e}^b = \mathbf{T}_q \mathbf{e}^q, \quad \hat{\mathbf{e}}^b = \hat{\mathbf{T}}_p \mathbf{e}^p, \tag{21}$$

with $\mathbf{T}_q$ and $\hat{\mathbf{T}}_p$ the *input trace matrices*.

4. By the properties of the matrices in (19) – details are omitted here and the reader is referred to [6] – the matrices $\mathbf{L}_q$ and $\mathbf{L}_p$ can be decomposed in order to define conjugated output maps

$$\mathbf{f}_0^b = \mathbf{S}_{p,0}\mathbf{e}^p, \quad \hat{\mathbf{f}}_0^b = \hat{\mathbf{S}}_{q,0}\mathbf{e}^q, \tag{22}$$

such that finally a finite-dimensional version of the balance equation (10) can be established:

$$\langle \mathbf{e}^p | \mathbf{M}_p \mathbf{f}^p \rangle + \langle \mathbf{e}^q | \mathbf{M}_q \mathbf{f}^q \rangle + \langle \mathbf{e}^b | \mathbf{f}_0^b \rangle + \langle \hat{\mathbf{e}}^b | \hat{\mathbf{f}}_0^b \rangle = 0. \tag{23}$$

5. The matrices $\mathbf{M}_p \in \mathbb{R}^{M_p \times N_p}$ and $\mathbf{M}_q \in \mathbb{R}^{M_q \times N_q}$ are non-square and/or rank-deficient. The discrete effort and flow degrees of freedom hence do not qualify to define a *finite-dimensional Dirac structure*, which approximates the original Stokes-Dirac structure. The reason is that the discrete efforts and flows that satisfy (20)-(22), define only as subset of the discrete (power) variables, for which the balance equation (23) is true[3].

A remedy is to determine mappings of the discrete flows and efforts with $\dim(\tilde{\mathbf{f}}^p) = \dim(\tilde{\mathbf{e}}^p)$ and $\dim(\tilde{\mathbf{f}}^q) = \dim(\tilde{\mathbf{e}}^q)$

$$\tilde{\mathbf{f}}^p = \mathbf{P}_{fp}\mathbf{f}^p, \ \tilde{\mathbf{f}}^q = \mathbf{P}_{fq}\mathbf{f}^q, \quad \tilde{\mathbf{e}}^p = \mathbf{P}_{ep}\mathbf{e}^p, \ \tilde{\mathbf{e}}^q = \mathbf{P}_{eq}\mathbf{e}^q, \tag{24}$$

as well as possibly modified conjugated output maps

$$\mathbf{f}^b = \mathbf{S}_p \mathbf{e}^p, \quad \hat{\mathbf{f}}^b = \hat{\mathbf{S}}_q \mathbf{e}^q, \tag{25}$$

such that they satisfy a balance equation

$$\langle \tilde{\mathbf{e}}^p | \tilde{\mathbf{f}}^p \rangle + \langle \tilde{\mathbf{e}}^q | \tilde{\mathbf{f}}^q \rangle + \langle \mathbf{e}^b | \mathbf{f}^b \rangle + \langle \hat{\mathbf{e}}^b | \hat{\mathbf{f}}^b \rangle = 0 \tag{26}$$

with non-degenerate duality products. The matrix condition, which results from substitution of (21), (24)-(25), and subsequently (20) in (26), is

$$(-1)^{n-1}\mathbf{d}_p^T \mathbf{P}_{fp}^T \mathbf{P}_{ep} + \mathbf{P}_{eq}^T \mathbf{P}_{fq} \mathbf{d}_q + \mathbf{T}_q^T \mathbf{S}_p + \hat{\mathbf{S}}_q^T \hat{\mathbf{T}}_p = \mathbf{0}. \tag{27}$$

Under the condition that $\dim(\tilde{\mathbf{e}}^p) + \dim(\tilde{\mathbf{e}}^q) + \dim(\mathbf{e}^b) + \dim(\hat{\mathbf{e}}^b) = M_p + M_q$ and

$$\mathrm{rank}(\begin{bmatrix} \mathbf{P}_{ep} \\ \hat{\mathbf{T}}_p \end{bmatrix}) = M_p, \quad \mathrm{rank}(\begin{bmatrix} \mathbf{P}_{eq} \\ \mathbf{T}_q \end{bmatrix}) = M_q, \tag{28}$$

[3]The subset of flows and efforts, which satisfy (20)-(22), is contained in its annihilator with respect to a symmetrized version of the duality product on the left hand side of (23). The reverse is not true. A Dirac structure is, however, defined as the subset of flows and efforts which coincides with its annihilator with respect to the mentioned symmetrized duality pairing.

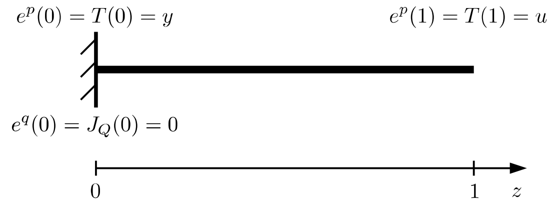

Fig. 1. Illustration of the 1D heat conductor with imposed boundary conditions $T(1) = u$ and $J_Q(0) = 0$ and the flat output $T(0) = y$.

the subspace of new discrete flow and effort variables is a *Dirac structure*, which admits the so-called *unconstrained in-/output representation*

$$\begin{aligned}\begin{bmatrix}-\tilde{\mathbf{f}}^p \\ -\tilde{\mathbf{f}}^q\end{bmatrix} &= \begin{bmatrix}\mathbf{0} & \mathbf{J}_p \\ \mathbf{J}_q & \mathbf{0}\end{bmatrix}\begin{bmatrix}\tilde{\mathbf{e}}^p \\ \tilde{\mathbf{e}}^q\end{bmatrix} + \begin{bmatrix}\mathbf{0} & \mathbf{B}_p \\ \mathbf{B}_q & \mathbf{0}\end{bmatrix}\begin{bmatrix}\hat{\mathbf{e}}^b \\ \mathbf{e}^b\end{bmatrix}, \\ \begin{bmatrix}\hat{\mathbf{f}}^b \\ \mathbf{f}^b\end{bmatrix} &= \begin{bmatrix}\mathbf{0} & \mathbf{B}_q^T \\ \mathbf{B}_p^T & \mathbf{0}\end{bmatrix}\begin{bmatrix}\tilde{\mathbf{e}}^p \\ \tilde{\mathbf{e}}^q\end{bmatrix} + \begin{bmatrix}\mathbf{0} & \mathbf{D}_q \\ \mathbf{D}_p & \mathbf{0}\end{bmatrix}\begin{bmatrix}\hat{\mathbf{e}}^b \\ \mathbf{e}^b\end{bmatrix},\end{aligned} \tag{29}$$

with

$$\begin{aligned}\begin{bmatrix}-\mathbf{J}_p & -\mathbf{B}_p \\ \mathbf{B}_q^T & \mathbf{D}_q\end{bmatrix} &= \begin{bmatrix}(-1)^{n-1}\mathbf{P}_{fp}\mathbf{d}_p \\ \hat{\mathbf{S}}_q\end{bmatrix}\begin{bmatrix}\mathbf{P}_{eq} \\ \mathbf{T}_q\end{bmatrix}^{-1}, \\ \begin{bmatrix}-\mathbf{J}_q & -\mathbf{B}_q \\ \mathbf{B}_p^T & \mathbf{D}_p\end{bmatrix} &= \begin{bmatrix}\mathbf{P}_{fq}\mathbf{d}_q \\ \mathbf{S}_p\end{bmatrix}\begin{bmatrix}\mathbf{P}_{ep} \\ \hat{\mathbf{T}}_p\end{bmatrix}^{-1}\end{aligned} \tag{30}$$

and $\mathbf{J}_p = -\mathbf{J}_q^T$, $\mathbf{D}_q = -\mathbf{D}_p^T$. For details see [6].

B. Constitutive equations and finite-dimensional dynamics

A consistent discretization of the constitutive equations (see the next section for the 1D heat equation and [6] for the 2D wave equation) leads to the discretized versions

$$\tilde{\mathbf{e}}^q = -\mathbf{Q}^q\tilde{\mathbf{f}}^q, \quad \tilde{\mathbf{e}}^p = \mathbf{Q}^p\tilde{\mathbf{p}} \tag{31}$$

of the two equations (12), where $\mathbf{Q}^q$ and $\mathbf{Q}^p$ are weighted discrete *Hodge* matrices. Together with the dynamics equation $\dot{\tilde{\mathbf{p}}} = -\mathbf{f}^p$, with $\tilde{\mathbf{p}}$ the vector of discrete state variables, we obtain the finite-dimensional approximation of the heat equation

$$\dot{\tilde{\mathbf{p}}} = -\mathbf{J}_q^T\mathbf{Q}_q\mathbf{J}_q\mathbf{Q}_p\tilde{\mathbf{p}} + \mathbf{J}_p\mathbf{Q}_q\mathbf{B}_q\hat{\mathbf{e}}^b + \mathbf{B}_p\mathbf{e}^b, \tag{32}$$

or in terms of the discrete temperature variable

$$\dot{\tilde{\mathbf{e}}}^p = -\mathbf{Q}_p\mathbf{J}_q^T\mathbf{Q}_q\mathbf{J}_q\tilde{\mathbf{e}}^p + \mathbf{Q}_p\mathbf{J}_p\mathbf{Q}_q\mathbf{B}_q\hat{\mathbf{e}}^b + \mathbf{Q}_p\mathbf{B}_p\mathbf{e}^b. \tag{33}$$

IV. STRUCTURE-PRESERVING DISCRETIZATION OF THE 1D HEAT EQUATION

A. Interconnection structure

The structured discretization of the heat equation on the interval $\Omega = (0, 1)$ using Whitney approximation forms[4], yields the numerical differentiation matrices

$$\mathbf{d}_p = \mathbf{d}_q = \begin{bmatrix}-1 & 1 & & \\ & \ddots & \ddots & \\ & & -1 & 1\end{bmatrix} \in \mathbb{R}^{N\times(N+1)}, \tag{34}$$

[4]Piecewise constant 1-forms (edges), piecewise linear 0-forms (nodes).

which describe the co-incidence relations between the N directed edges and $N{+}1$ nodes on the discretization grid. The flow degrees of freedom $\mathbf{f}^p$ and $\mathbf{f}^q$ have the interpretation of the rate of change of internal energy and the temperature difference on the N edges of the grid, while $\mathbf{e}^p$ and $\mathbf{e}^q$ are temperatures and heat fluxes, localized in the $N+1$ nodes.

Designating the efforts $e^p(1)$ and $e^q(0)$ as boundary inputs translates to the definition of $1 \times (N{+}1)$ input trace matrices

$$\hat{\mathbf{T}}_p = \begin{bmatrix}0 & \cdots & 0 & 1\end{bmatrix}, \quad \mathbf{T}_q = \begin{bmatrix}1 & 0 & \cdots & 0\end{bmatrix}. \tag{35}$$

With the mappings

$$\mathbf{P}_{ep} = \begin{bmatrix}\mathbf{I}_N & \mathbf{0}_{N\times 1}\end{bmatrix}, \qquad \mathbf{P}_{eq} = \begin{bmatrix}\mathbf{0}_{N\times 1} & \mathbf{I}_N\end{bmatrix}, \tag{36}$$

the remaining nodal efforts are collected in the vectors $\tilde{\mathbf{e}}^p, \tilde{\mathbf{e}}^q \in \mathbb{R}^N$, and the matrices

$$\begin{bmatrix}\mathbf{P}_{eq} \\ \mathbf{T}_q\end{bmatrix}^T = \begin{bmatrix}\mathbf{P}_{eq} \\ \mathbf{T}_q\end{bmatrix}^{-1}, \qquad \begin{bmatrix}\mathbf{P}_{ep} \\ \hat{\mathbf{T}}_p\end{bmatrix}^T = \begin{bmatrix}\mathbf{P}_{ep} \\ \hat{\mathbf{T}}_p\end{bmatrix}^{-1} \tag{37}$$

become permutation matrices, which avoids inversion when computing the matrices (30) of the input-output representation of the finite-dimensional Dirac structure. The flow maps

$$\mathbf{P}_{fp} = \mathbf{P}_{fq}^T = \begin{bmatrix}1-\alpha & & & \\ \alpha & 1-\alpha & & \\ & \ddots & \ddots & \\ & & \alpha & 1-\alpha\end{bmatrix} \tag{38}$$

and the definition of conjugated discrete outputs

$$\begin{aligned}\hat{\mathbf{S}}_q &= \begin{bmatrix}0 & \cdots & 0 & -\alpha & \alpha-1\end{bmatrix}, \\ \mathbf{S}_p &= \begin{bmatrix}1-\alpha & \alpha & 0 & \cdots 0\end{bmatrix}\end{aligned} \tag{39}$$

complete the parametrization of mappings such that the matrix equation (27) is satisfied. $\alpha \in \mathbb{R}$ is a free design parameter which can be used to tune the resulting numerical approximation while the *structure remains preserved*.

The subspace of so-defined *minimal* flows and efforts, which satisfy the discrete structure equation (29), is a Dirac structure, which approximates the infinite-dimensional Stokes-Dirac structure. The evaluation of (30) yields the $n\times n$ interconnection matrices

$$\mathbf{J}_p = -\mathbf{J}_q^T = \begin{bmatrix}\alpha-1 & & & \\ 1-2\alpha & \alpha-1 & & \\ \alpha & 1-2\alpha & \alpha-1 & \\ & \ddots & \ddots & \ddots \\ & \alpha & 1-2\alpha & \alpha-1\end{bmatrix} \tag{40}$$

and the $N \times 1$ *input matrices*

$$\mathbf{B}_p = \mathbf{S}_p^T, \quad \mathbf{B}_q = \hat{\mathbf{S}}_q^T. \tag{41}$$

Remark 3: For the considered Whitney forms, the discrete flow variables $\mathbf{f}^p, \mathbf{f}^q \in \mathbb{R}^N$ can be interpreted as approximate line integrals of the one-forms f^p and f^q over the directed edges. By the mappings $\mathbf{P}_{fp}$ and $\mathbf{P}_{fq}$, the elements of $\tilde{\mathbf{f}}^p, \tilde{\mathbf{f}}^q \in \mathbb{R}^N$ become convex sums of discrete flow variables on neighboring edges. Exceptions are the first and the last element $\tilde{f}_1^p = (1-\alpha)f_1^p$ and $\tilde{f}_N^q = (1-\alpha)f_N^q$ with a weight different from 1 if $\alpha \neq 0$. This difference must be considered in the consistent approximation of the constitutive equations.

TABLE I
DIMENSIONS OF FLOW AND EFFORT VECTORS ON THE 1D GRID

Vector(s)	$\mathbf{f}^p, \mathbf{f}^q$	$\mathbf{e}^p, \mathbf{e}^q$	$\mathbf{e}^b, \mathbf{f}^b$	$\hat{\mathbf{e}}^b, \hat{\mathbf{f}}^b$	$\tilde{\mathbf{f}}^p, \tilde{\mathbf{e}}^p$	$\tilde{\mathbf{f}}^q, \tilde{\mathbf{e}}^q$
Dimension	N	$N+1$	1	1	N	N

B. Constitutive equations

According to (36), the *co-state* vector $\tilde{\mathbf{e}}^p$ contains the temperatures at the nodes $1, \ldots, N$. Assuming a constant isochoric heat capacity c_v, a constant temperature profile with $\tilde{e}^p_j = \bar{e}^p = const.$, $j = 1, \ldots, N$ corresponds to the discrete internal energies

$$\tilde{p}_i = \frac{c_v}{N} \sum_{j=1}^{N} [\mathbf{P}_{fp}]_{ij} \bar{e}^p, \qquad i = 1, \ldots, N. \tag{42}$$

A consistent discretization of the calorimetric equation based on this steady state is

$$\tilde{\mathbf{p}} = \frac{c_v}{N} \mathrm{diag}\{1-\alpha, 1, \ldots, 1\} \, \tilde{\mathbf{e}}^p. \tag{43}$$

The factor $1-\alpha$ scales the state $\tilde{p}_1$ at the left boundary compared to $\tilde{p}_2, \ldots, \tilde{p}_N$ in a constant equilibrium state. Equivalently, we have

$$\tilde{\mathbf{e}}^p = \mathbf{Q}_p \tilde{\mathbf{p}} \quad \text{with} \quad \mathbf{Q}_p = \frac{N}{c} \begin{bmatrix} \frac{1}{1-\alpha} & & & \\ & 1 & & \\ & & \ddots & \\ & & & 1 \end{bmatrix}. \tag{44}$$

If $\tilde{\mathbf{f}}^q$ is the vector of discrete thermodynamic driving forces, then it contains temperature differences along the edges, weighted by the elements of $\mathbf{P}_{fq}$. The consistent computation of the discrete heat fluxes in the nodes $2, \ldots, N+1$ from the vector of driving forces is performed via

$$\tilde{\mathbf{e}}^q = -\mathbf{Q}_q \tilde{\mathbf{f}}^q \quad \text{with} \quad \mathbf{Q}_q = \lambda N \begin{bmatrix} 1 & & & \\ & \ddots & & \\ & & 1 & \\ & & & \frac{1}{1-\alpha} \end{bmatrix}, \tag{45}$$

with a constant assumed heat conductivity λ. As for the calorimetric equation, this discrete relation is derived from considering Fourier's law with constant heat fluxes $\tilde{e}^q_j = \bar{e}^q = const.$, $j = 1, \ldots, N$. In this case,

$$\sum_{j=1}^{N} [\mathbf{P}_{fq}]_{ij} \bar{e}^q = -\lambda N \tilde{f}^q_i \tag{46}$$

holds, from which the above relation follows. Again, the different last element of $\mathbf{Q}_q$ accounts for the scaling of $\tilde{f}^q_N$ compared to $\tilde{f}^q_1, \ldots, \tilde{f}^q_{N-1}$ when constant temperature differences $f^q_1, \ldots f^q_N$ on the original discretization intervals are considered.

C. State space model

Considering the boundary conditions

$$\hat{e}^b = \hat{\mathbf{T}}_p \mathbf{e}^p = u, \qquad e^b = \mathbf{T}_q \mathbf{e}^q = 0, \tag{47}$$

as illustrated in Fig. 1, and denoting $\mathbf{x} := \tilde{\mathbf{p}} \in \mathbb{R}^N$ the state vector of weighted internal energies on the discretization intervals, we obtain the finite-dimensional state differential equation for the heat equation according to (32)

$$\dot{\mathbf{x}} = \mathbf{A}\mathbf{x} + \mathbf{b}u \tag{48}$$

with

$$\mathbf{A} = -\mathbf{J}_q^T \mathbf{Q}_q \mathbf{J}_q \mathbf{Q}_p, \qquad \mathbf{b} = \mathbf{J}_p \mathbf{Q}_q \mathbf{B}_q. \tag{49}$$

Multiplication of the solution $\mathbf{x}$ with the Hodge matrix $\mathbf{Q}_p$ gives the vector of temperatures $\mathbf{e} = \mathbf{Q}_p \mathbf{x}$ in the nodes $1, \ldots, N-1$. As we are interested in the *feedforward control problem* for the temperature $T(0)$, the corresponding output equation is

$$y = \mathbf{c}^T \mathbf{x} \tag{50}$$

with

$$\mathbf{c}^T = \begin{bmatrix} 1 & 0 & \ldots & 0 \end{bmatrix} \mathbf{Q}_p. \tag{51}$$

The state matrix $\mathbf{A}$ is symmetric and pentadiagonal,

$$\begin{aligned} \mathbf{A} = \mathrm{diag}(\mathbf{a}_0) + \mathrm{diag}_1(\mathbf{a}_1) + \mathrm{diag}_{-1}(\mathbf{a}_1) \\ + \mathrm{diag}_2(\mathbf{a}_2) + \mathrm{diag}_{-2}(\mathbf{a}_2), \end{aligned} \tag{52}$$

with the vectors of main diagonal elements $\mathbf{a}_0 \in \mathbb{R}^N$ and the elements on the first two upper and lower off-diagonals $\mathbf{a}_1 \in \mathbb{R}^{N-1}$ and $\mathbf{a}_2 \in \mathbb{R}^{N-2}$,

$$\begin{aligned} \mathbf{a}_0 &= N^2 \left[-1+\alpha,\ -2+6\alpha-5\alpha^2,\ -2+6\alpha-6\alpha^2,\ \ldots,\right. \\ &\qquad \left. -2+6\alpha-6\alpha^2,\ -2+5\alpha-5\alpha^2\right], \\ \mathbf{a}_1 &= N^2 \left[1-3\alpha+2\alpha^2,\ 1-4\alpha+4\alpha^2,\ \ldots,\ 1-4\alpha+4\alpha^2\right], \\ \mathbf{a}_2 &= N^2 \left[\alpha-\alpha^2,\ \ldots,\ \alpha-\alpha^2\right]. \end{aligned} \tag{53}$$

The input vector is

$$\mathbf{b} = N \left[0,\ \ldots\ 0,\ \alpha-\alpha^2,\ 1-2\alpha+2\alpha^2\right]^T. \tag{54}$$

$\mathbf{a}_1$ and $\mathbf{a}_2$ become zero vectors for the cases $\alpha = \frac{1}{2}$ and $\alpha = 0$, respectively. These two cases will be analyzed in the following section.

V. APPROXIMATION QUALITY OF THE NUMERICAL MODELS

We compare the properties of the discretized model to those of the infinite-dimensional one. In particular, we are interested in a) the approximation of the eigenvalues of the system operator and b) the possibility to parametrize the input $u = T(1)$ (and the state) by the desired flat output $y = T(0)$ and its time derivatives. We consider the case of constant material parameters $\frac{\lambda}{c_v} = 1$.

A. Properties of the PDE model

To analyze the eigenvalues, we write the 1D heat equation on $(0, 1) \subset \mathbb{R}$ with *homogeneous* boundary conditions:

$$\partial_t x(z,t) = \partial_z^2 x(z,t), \quad \partial_z x(0,t) = 0,\ x(1,t) = 0. \tag{55}$$

It is easily verified, that an initial condition in the form

$$x(z,0) = \sum_{k=1}^{\infty} c_k \cos(\sqrt{-\lambda_k} z) \tag{56}$$

with the negative real *eigenvalues*

$$\lambda_{k,\infty} = -\left(\frac{2k-1}{2}\pi\right)^2, \quad k = 1, 2, \dots \tag{57}$$

decays according to

$$x(z,t) = \sum_{k=1}^{\infty} c_k e^{\lambda_k t} \cos(\sqrt{-\lambda_k} z). \tag{58}$$

The Laplace transformation of the heat equation allows to establish a transfer function between the input $\hat{u}(s) = \hat{x}(1,s)$ and the output $\hat{y}(s) = \hat{x}(0,s)$ as

$$\hat{y}(s) = \frac{1}{\cosh(\sqrt{s})}\hat{u}(s), \tag{59}$$

which allows, via a series expansion of $\cosh(\sqrt{s})$ and backtransformation to the time domain a *flat parametrization* of the input

$$u(t) = \sum_{j=0}^{\infty} \frac{1}{(2j)!}\partial_t^j y(t). \tag{60}$$

Choosing an infinitely often differentiable *smooth step function* of *Gevrey order* in the open interval $(1,2)$ for the desired output $y(t)$, the convergence of the series is guaranteed and a flatness-based feedforward control can be determined [9].

B. Approximate eigenvalues and zeros

Based on the structure of the matrices $\mathbf{A}$, $\mathbf{b}$ and $\mathbf{c}^T$, we first analyze the eigenvalues and possible zeros of the state space model (48), (50) for the two cases $\alpha = 0$ and $\alpha = \frac{1}{2}$.

1) $\alpha = 0$: The matrices $\mathbf{A}$, $\mathbf{b}$ and $\mathbf{c}^T$ have the structure

$$\mathbf{A} = N^2\mathbf{X} = N^2 \begin{bmatrix} -1 & 1 & & \\ 1 & -2 & \ddots & \\ & \ddots & \ddots & 1 \\ & & 1 & -2 \end{bmatrix},$$
$$\mathbf{b} = N \begin{bmatrix} 0 \\ \vdots \\ 0 \\ 1 \end{bmatrix}, \quad \mathbf{c}^T = N \begin{bmatrix} 1, & 0, & \dots, & 0 \end{bmatrix}. \tag{61}$$

The roots λ_k, $k = 1, \dots, N$ of the characteristic polynomial $p(\lambda) = \det(\lambda\mathbf{I} - \mathbf{A})$ are the roots λ'_k of $p'(\lambda') = \det(\lambda'\mathbf{I} - \mathbf{X})$, multiplied with N^2. The tridiagonal form of $\mathbf{X}$ allows to construct the characteristic polynomial by recursion of the determinants of south-eastern submatrices. This recursion resembles the one for the Chebyshev polynomials of the first kind. With the changes of variables $\lambda' + 2 = 2\mu$ and $\mu = \cos(\eta)$, one finds the roots of p'

$$\eta_k = \frac{2k-1}{2N+1}\pi, \qquad k = 1, \dots, N, \tag{62}$$

and finally the eigenvalues of $\mathbf{A}$

$$\lambda_k = 2N^2\left(\cos(\frac{2k-1}{2N+1}\pi) - 1\right), \quad k = 1, \dots, N. \tag{63}$$

The invariant zeros are the roots of $\det(\mathbf{P}(\eta))$ with

$$\mathbf{P}(\eta) = \begin{bmatrix} \mathbf{A} - \eta\mathbf{I} & \mathbf{b} \\ \mathbf{c}^T & 0 \end{bmatrix} \tag{64}$$

the Rosenbrock matrix. A short calculation shows that

$$\det(\mathbf{P}(\eta)) = (-1)^N N^4 \det([\mathbf{X} - \eta\mathbf{I}]_{1:N-1,2:N}) = (-1)^N N^4, \tag{65}$$

where $[\mathbf{X} - \eta\mathbf{I}]_{1:N-1,2:N}$ denotes the $(N-1) \times (N-1)$ north-eastern submatrix of $\mathbf{X} - \eta\mathbf{I}$, which is lower triangular. The discretized models $(\mathbf{A}, \mathbf{b}, \mathbf{c}^T)$ with parameter $\alpha = 0$ have no invariant zeros. Thus, the output has full relative degree N. It is a flat output, as the input and the states can be parametrized in terms of $y(t)$ and its time derivatives, which allows to compute a feedforward control $u(t)$ as in the infinite-dimensional case.

The presented discretization of the heat equation conserves not only the interconnection structure and approximates the eigenvalues asymptotically, but also preserves the flatness of the output $y(t)$.

2) $\alpha = \frac{1}{2}$: The $\mathbf{A}$ matrix has a chessboard pattern. We assume an even number N of discretization intervals. The non-zero elements of $\mathbf{A}$ can be collected in the matrix $\mathbf{A}_1 := [\mathbf{A}]_{1:2:N-1,1:2:N-1}$ of odd rows and columns and the matrix $\mathbf{A}_2 := [\mathbf{A}]_{2:2:N,2:2:N}$ of even rows and columns:

$$\mathbf{A}_1 = \left(\frac{N}{2}\right)^2 \begin{bmatrix} -2 & 1 & & & \\ 2 & -2 & 1 & & \\ & 1 & -2 & \ddots & \\ & & \ddots & \ddots & 1 \\ & & & 1 & -2 \end{bmatrix},$$
$$\mathbf{A}_2 = \left(\frac{N}{2}\right)^2 \begin{bmatrix} -1 & 1 & & & \\ 1 & -2 & \ddots & & \\ & \ddots & \ddots & 1 & \\ & & 1 & -2 & 1 \\ & & & 1 & -3 \end{bmatrix}. \tag{66}$$

Both matrices are similar, they are related via the equality $\mathbf{A}_1\mathbf{S} = \mathbf{S}\mathbf{A}_2$ with the upper triangular matrix

$$\mathbf{S} = \begin{bmatrix} 1 & -1 & 1 & \cdots & \\ & 2 & -2 & \cdots & \\ & & \ddots & \ddots & \\ & & & 2 & -2 \\ & & & & 2 \end{bmatrix}, \tag{67}$$

whose elements have alternating sign. Consequently, $\mathbf{A}_1$ and $\mathbf{A}_2$ have identical eigenvalues. The analysis of the characteristic polynomial of $\mathbf{A}_2$, with the help of the recurrence relation for Chebyshev polynomials, results in the eigenvalues

$$\lambda_k = \frac{N^2}{2}\left(\cos(\frac{2k-1}{N}\pi) - 1\right), \qquad k = 1, \dots, \frac{N}{2}. \tag{68}$$

These eigenvalues of $\mathbf{A}_1$ (and by similarity of $\mathbf{A}_2$) represent eigenvalues of the complete state matrix $\mathbf{A}$ with algebraic multiplicity 2.

Defining the partial state vectors $\mathbf{x}_1 := [\mathbf{x}]_{1:2:N-1}$ and $\mathbf{x}_2 := [\mathbf{x}]_{2:2:N}$, the system (48), (50) for $\alpha = \frac{1}{2}$ can be written

$$\begin{bmatrix}\dot{\mathbf{x}}_1\\ \dot{\mathbf{x}}_2\end{bmatrix} = \begin{bmatrix}\mathbf{A}_1 & \mathbf{0}\\ \mathbf{0} & \mathbf{A}_2\end{bmatrix}\begin{bmatrix}\mathbf{x}_1\\ \mathbf{x}_2\end{bmatrix} + \begin{bmatrix}\mathbf{b}_1\\ \mathbf{b}_2\end{bmatrix} u,$$
$$y = \begin{bmatrix}\mathbf{c}_1^T & \mathbf{c}_2^T\end{bmatrix}\begin{bmatrix}\mathbf{x}_1\\ \mathbf{x}_2\end{bmatrix}, \tag{69}$$

with

$$\mathbf{b}_1 = N\begin{bmatrix}0\\ \vdots\\ 0\\ \frac{1}{4}\end{bmatrix}, \quad \mathbf{b}_2 = N\begin{bmatrix}0\\ \vdots\\ 0\\ \frac{1}{2}\end{bmatrix}, \tag{70}$$
$$\mathbf{c}_1^T = N\begin{bmatrix}2,\ 0,\ \dots,\ 0\end{bmatrix}, \quad \mathbf{c}_2^T = \mathbf{0}^T.$$

The subsystem

$$\begin{aligned}\dot{\mathbf{x}}_1 &= \mathbf{A}_1\mathbf{x}_1 + \mathbf{b}_1 u\\ y &= \mathbf{c}_1^T\mathbf{x}_1\end{aligned} \tag{71}$$

has no invariant zero, i. e. $y(t)$ has relative degree $\frac{N}{2}$ and represents a flat output for this subsystem. A feedforward control $u(t)$ can be computed based on the inversion of the transfer function $G_1(s) = \mathbf{c}_1^T(s\mathbf{I}-\mathbf{A})^{-1}\mathbf{b}_1$, only taking into account $y(t)$ and its time derivatives up to order $\frac{N}{2}$.

The control $u(t)$ excites the stable internal dynamics

$$\dot{\mathbf{x}}_2 = \mathbf{A}_2\mathbf{x} + \mathbf{b}_2 u, \tag{72}$$

whose eigenvalues (i. e. one half of the eigenvalues of $\mathbf{A}$) coincide with the invariant zeros.

C. Convergence of the eigenvalues

We replace the cosines in the discretized eigenvalue expressions (63) and (68) by their series expansions and obtain for $\alpha = 0$ (see also [8] for this case)

$$\lambda_k = \lambda_{k,\infty}\left(1 - \frac{1}{N} + o\big(\frac{1}{N}\big)\right) \tag{73}$$

and for $\alpha = \frac{1}{2}$

$$\lambda_k = \lambda_{k,\infty}\left(1 + \frac{2\lambda_{k,\infty}}{4!\left(\frac{N}{2}\right)^2} + o\big(\frac{1}{\left(\frac{N}{2}\right)^2}\big)\right). \tag{74}$$

We conclude that the eigenvalues of the heat equation are approximated with a first order error for $\alpha = 0$ and an error of second order for $\alpha = \frac{1}{2}$.

Remark 4: The result that $\alpha = \frac{1}{2}$ provides a superior approximation of the eigenvalues supports the observation that a comparable parametrization of the discretization according to [3] (also with a parameter value of $\frac{1}{2}$) yields excellent results for diffusive systems, see [4]. Note however that in [3], the mappings of the nodal efforts are parametrized (while this is the case for the edge flows in our approach). This gives triangular instead of banded matrices $\mathbf{J}_p = -\mathbf{J}_q^T$, which hampers a simple representation of the discretized eigenvalues and their subsequent convergence analysis for $N \to \infty$. Moreover, parametrized mappings of the discrete flows instead of the efforts allow for a straightforward extension to higher spatial dimensions, see [6].

D. Simulations

We present a series of simulations that support our results concerning the quality of the finite-dimensional approximations of the 1D heat equation and their usability for flatness-based feedforward control.

1) Initial value problem: In Fig. 2, we compare the *numerical* solution of the heat equation under Neumann-Dirichlet boundary conditions (55) with initial condition (only third mode)

$$x_0(t) = x(z,0) = \cos(\frac{5}{2}\pi z), \tag{75}$$

with the exact solution at time $t_e = \ln 4/\left(\frac{5}{2}\pi\right)^2$,

$$x(z,t_e) = e^{-\frac{25}{4}\pi^2 t_e} x_0(z) = \frac{1}{4}x_0(z). \tag{76}$$

While for $\alpha = 0$, the error over z is reduced by a factor 2 when doubling the number of discretization intervals from $N = 40$ to $N = 80$, we note that the approximation with $\alpha = \frac{1}{2}$ and $N = 40$ is superior in terms of error magnitude and shape, which resembles the considered third mode.

2) Flatness-based feedforward control: For the numerical experiments, we use a simulation model with $\alpha = \frac{1}{2}$, $N_{sim} = 160$, which is integrated using Matlab's lsim with a time step of 10^{-5}. We consider as reference output $y^*(t) = x^*(0,t)$ a transient between $y(0) = 0$ and $y(1) = 1$, which is described by a Gevrey class function as in [9]. We use the parameter $\gamma = 1.1$, which leads to Gevrey order $1 - \frac{1}{1.1} < 2$. The infinite series (60) to compute the flat input parametrization is cut after the 10th time derivative of $y^*(t)$. The corresponding controller is denoted $u_\infty^{10}(t)$. For comparison, we compute the feedforward control based on the inversion of the transfer functions $\mathbf{c}^T(s\mathbf{I}-\mathbf{A})^{-1}\mathbf{b}$ for $\alpha = 0$ and $\mathbf{c}_1^T(s\mathbf{I}-\mathbf{A}_1)^{-1}\mathbf{b}_1$ for $\alpha = \frac{1}{2}$. The time domain expression for $u^*(t)$ is a finite weighted sum of $y^*(t)$ and its time derivatives, which is also cut after the first 10 (or 5, respectively) time derivatives. The corresponding controllers are denoted $u_N^{5/10}(t)$, where the subscript denotes the order N of the control design model and the superscript the number of time derivatives of the flat output that were used.

Figure 3 illustrates the solution $\mathbf{e}^p(\mathbf{z},t) = \mathbf{Q}_p\tilde{\mathbf{p}}(t)$ over space and time of the temperature transient with input $u_{40}^{10}(t)$. In Fig. 4, we compare the simulated output with the reference trajectory for $\alpha = 0$ (top) and $\alpha = \frac{1}{2}$ (bottom), under variation of $N \in \{40, 80\}$ and the number of used output derivatives (10 or 5). The different order (1 vs. 2) of the approximation error is evident from the curves and also the decreasing effect of higher order derivatives of the flat output can be observed, comparing the solid with the dotted curves.

VI. CONCLUSIONS

We presented the application of a structure-preserving discretization scheme to the nD heat equation. For the 1D case, we analyzed the structure of the finite-dimensional approximate state space models for two representative parameter values, for which expressions on the order of the eigenvalue approximation error could be derived. We showed

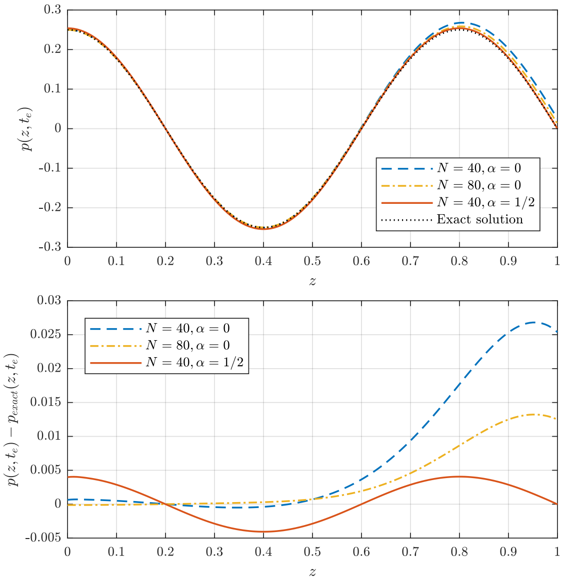

Fig. 2. Top: Exact and numerical solutions of the initial value problem for the heat equation. Bottom: Errors between numerical and exact solution for different parametrizations.

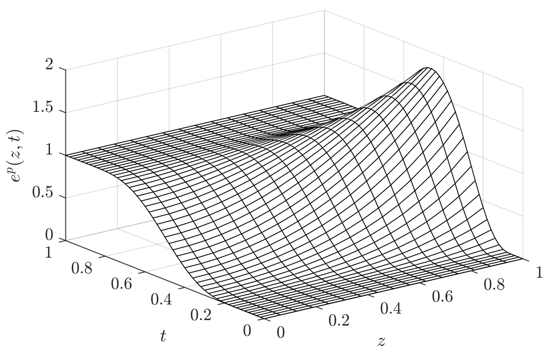

Fig. 3. Simulation result with the feedforward controller for predefined s-shaped transient of $y = T(0) = e^p(0)$ with $\gamma = 1.1$, corresponding to Gevrey order $1 + \frac{1}{1.1} < 2$. Controller design: $N = 40$, $\alpha = \frac{1}{2}$, using y and its time derivatives up to order 10. Simulation: $N_{sim} = 160$, $\alpha = \frac{1}{2}$.

that the flatness of a given output (the temperature at the isolated end of the heat conductor), i. e. the possibility to parametrize inputs and states by the output and its time derivatives, is conserved for the parameter value $\alpha = 0$, which corresponds to a one-sided approximation of the constitutive equations. The parameter value $\alpha = \frac{1}{2}$ (centered approximation of the constitutive equations) is preferable in terms of approximation quality. It allows also for a flat parametrization of the input, although one half of the states is obtained by integration of the asymptotically stable internal dynamics. The feedforward control based on this finite-dimensional approximation model shows high quality, with the second order of the approximation error confirmed by simulations under grid refinement.

In ongoing works we exploit the insights concerning the structure-preserving discretization of hyperbolic and parabolic systems of conservation laws for the simulation and computational control of mass and heat transfer phenomena in three-dimensional heterogeneous media.

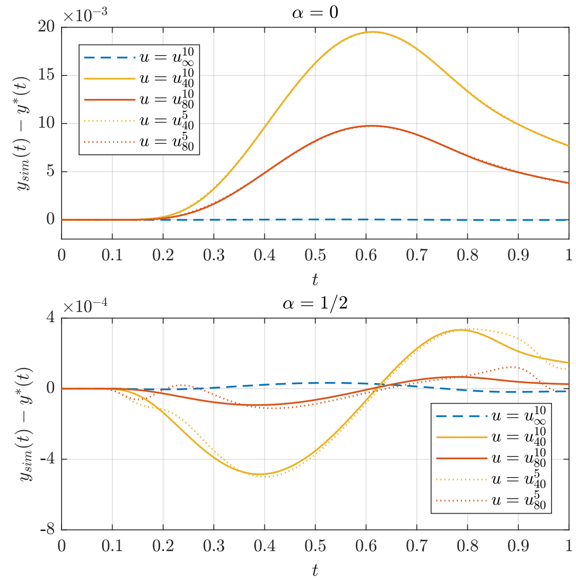

Fig. 4. Output errors under flatness-based feedforward control, with the simulation model with $N_{sim} = 160$, $\alpha = \frac{1}{2}$. u_c^{10}: Analytic computation of feedforward control using 10 time derivatives of y. $u_{40/80}^{5/10}$: Computation of the feedforward control based on the discretized model with $\alpha = \frac{1}{2}$, $N = 40$ of 80 and using 5 or 10 time derivatives of the desired output.

References

[1] V. Duindam, A. Macchelli, S. Stramigioli, and H. Bruyninckx, *Modeling and Control of Complex Physical Systems: The Port-Hamiltonian Approach*. Springer, 2009.

[2] A. J. van der Schaft and B. M. Maschke, "Hamiltonian formulation of distributed-parameter systems with boundary energy flow," *Journal of Geometry and Physics*, vol. 42, no. 1, pp. 166–194, 2002.

[3] G. Golo, V. Talasila, A. van der Schaft, and B. Maschke, "Hamiltonian discretization of boundary control systems," *Automatica*, vol. 40, no. 5, pp. 757–771, May 2004.

[4] A. Baaiu, F. Couenne, L. Lefevre, Y. Le Gorrec, and M. Tayakout, "Structure-preserving infinite dimensional model reduction: Application to adsorption processes," *Journal of Process Control*, vol. 19, no. 3, pp. 394–404, 2009.

[5] R. Moulla, L. Lefèvre, and B. Maschke, "Pseudo-spectral methods for the spatial symplectic reduction of open systems of conservation laws," *Journal of Computational Physics*, vol. 231, no. 4, pp. 1272–1292, 2012.

[6] P. Kotyczka, B. Maschke, and L. Lefèvre, "Weak form of Stokes-Dirac structures and geometric discretization of port-Hamiltonian systems," *Journal of Computational Physics*, vol. 361, pp. 442–476, 2018.

[7] H. Whitney, "Geometric integration theory," *Princeton UP, Princeton*, 1957.

[8] Y. Le Gorrec, H. Peng, L. Lefèvre, B. Hamroun, and F. Couenne, "Systèmes hamiltoniens à ports de dimension infinie: réduction et propriétés spectrales." *Journal Européen des Systèmes Automatisés (JESA)*, vol. 45, no. 7-10, pp. 645–664, 2011.

[9] B. Laroche, P. Martin, P. Rouchon, *et al.*, "Motion planning for the heat equation," *International Journal of Robust and Nonlinear Control*, vol. 10, no. 8, pp. 629–643, 2000.

[10] H. Flanders, *Differential Forms with Applications to the Physical Sciences*. Academic Press New York, 1963, vol. 197, no. 3.

[11] H. Brezis, *Functional analysis, Sobolev spaces and partial differential equations*. Springer Science & Business Media, 2011.

[12] D. Arnold, R. Falk, and R. Winther, "Finite element exterior calculus: from Hodge theory to numerical stability," *Bulletin of the American Mathematical Society*, vol. 47, no. 2, pp. 281–354, 2010.

[13] D. D. Holm, *Geometric mechanics: Part 1: Dynamics and symmetry*. Imperial College Press, 2011.

[14] D. N. Arnold, "Spaces of finite element differential forms," in *Analysis and numerics of partial differential equations*. Springer, 2013, pp. 117–140.